Proceedings of the 2014 IEEE
International Conference on Robotics and Biomimetics
December 5-10, 2014, Bali, Indonesia

Ceiling Vision Localization with Feature Pairs for Home Service Robots

Pengjin Chen, Zhaopeng Gu*, Guodong Zhang, Hong Liu

***Abstract*— Automatically self-localization of home service robot in indoor environments is a key issue with high efficiency and robustness. State-of-the-art frameworks in computer vision typically are based on Simultaneous Localization And Mapping (SLAM) and extended version such as Ceiling Vision SLAM (CV-SLAM). However, a large amount of map information about landmarks in the ceiling are redundant for home service robots only to accomplish the localization task such as indoor cleaning robot. In this paper, a fast and robust ceiling vision localization framework based on CV-SLAM is proposed, which consists of three parts: ceiling features operation, localization with feature pairs and visual odometry. In addition, we propose a novel localization method with feature pairs based on ceiling vision, which can enhance the real-time capability effectively. Simulation and real experiments validate the efficiency of our approach for the localization tasks of home service robots in indoor environments.**

***Index Terms*— Localization, SLAM, Ceiling vision, Home service robot.**

I. Introduction

In recent years, home service robots have attracted extensive attention in both scientific research and industrial fields, such as robotic vacuum cleaners and social robots. When service robots execute their missions automatically, self-localization is a fundamental need. Position information is vital for decision making and path planning, while self-localization requires lower time consumption and higher accuracy in real applications.

Traditionally, active range sensors have been applied for data association such as sonar or laser scanner in most localization algorithms. These localization frameworks based on active sensors still have limitations in cost and applicability. However, the methods based on computer vision have great advantages compared with active range sensors in low cost and fast speed. Therefore, a variety of approaches for localization tasks based on vision sensors have been proposed. Hereby, these approaches can summarily be classified into two categories: monocular camera and stereo camera.

In this paper, the former category is to draw more close attention. For the monocular camera field, existing works can be further classified into two categories which are feature based methods and appearance based methods. Nister et al. [1] illustrated the excellent results of visual odometry estimation which employed a five-point solver to figure out ego-motion using RANdom SAmple Consensus (RANSAC) with a single camera. In 2D localization and mapping aspect, Whyte and Bailey [2] provided an overview of the recent achievements in Simultaneous Localization And Mapping (SLAM).

SLAM is a significant issue in autonomous robots field, and a great deal of researches have been conducted on indoor SLAM [3, 4, 5] using sensors [6], features, and filters [7, 8]. In practice, sensors and filtering methods are combined which applied in the SLAM problems. Davison et al. [4] demonstrated the implementation of a monocular camera SLAM, which using a six degrees of freedom handheld camera. In MonoSLAM [4], the corner points of salient visual patches were registered as landmarks. Next, the motion of camera was predicted by the constant velocity model, and the landmarks were initialized by inverse depth estimation [11] and tracked by Extended Kalman Filter (EKF). In addition, Frintrop et al. [10] introduced an active gaze-control system which tracked salient features using a pan-tilt camera, and it can track existing features actively and prepare for loop closures ahead of time.

More recently, there are considerable progresses on Ceiling Vision based SLAM (CV-SLAM) [15, 16, 18]. Jeong et al. [9] first presented CV-SLAM, where corner points were detected by the Harris corner detector and their orientations as well as their positions were estimated. However, Jeong's approaches did not reflect that the two landmarks shared similar information and the inclusion of both landmarks in the state vector may bring more inefficiency to some extent. Afterwards, Hwang et al. [8] proposed a novel monocular vision based CV-SLAM , which detected corners and lamps on ceilings and doors from ceiling images and builded a map of multiple types of landmarks. Choi et al. [12] utilized the ceiling boundary feature map approach in SLAM, since the ceiling boundaries were robust to illuminative variations and they were not as numerous as the point features.

In CV-SLAM, ceiling images have huge advantages that they are extremely static, rarely occluded, well-structured and less disturbance from environment noises. Furthermore, they have more repetitive patterns and detect far fewer landmarks compared to front images from forward-looking cam-

This work is supported by National Natural Science Foundation of China (NSFC, No.60875050, 60675025, 61340046), National High Technology Research and Development Program of China (863 Program, No.2006AA04Z247), Science and Technology Innovation Commission of Shenzhen Municipality (No.201005280682A, No.JCYJ20120614152234873), the Specialized Research Fund for the Doctoral Program of Higher Education (No. 20130001110011).

Pengjin Chen is with the Engineering Lab on Intelligent Perception for Internet of Things(ELIP), Shenzhen Graduate School, Peking University, Shenzhen, 518055 CHINA. chenpengjin@gmail.com

Zhaopeng Gu is with the Engineering Lab on Intelligent Perception for Internet of Things(ELIP), Shenzhen Graduate School, Peking University, Shenzhen, 518055 CHINA. guzp@pkusz.edu.cn

Guodong Zhang is with the Shenzhen Silver Star Intelligent Technology Co., LTD, Shenzhen, 518055 CHINA. johnson@yxrobot.net

Hong Liu is with the Engineering Lab on Intelligent Perception for Internet of Things(ELIP), and the Key Laboratory of Machine Perception, Peking University, Beijing, 100087 CHINA. hongliu@pku.edu.cn

978-1-4799-7397-2/14/$31.00 © 2014 IEEE

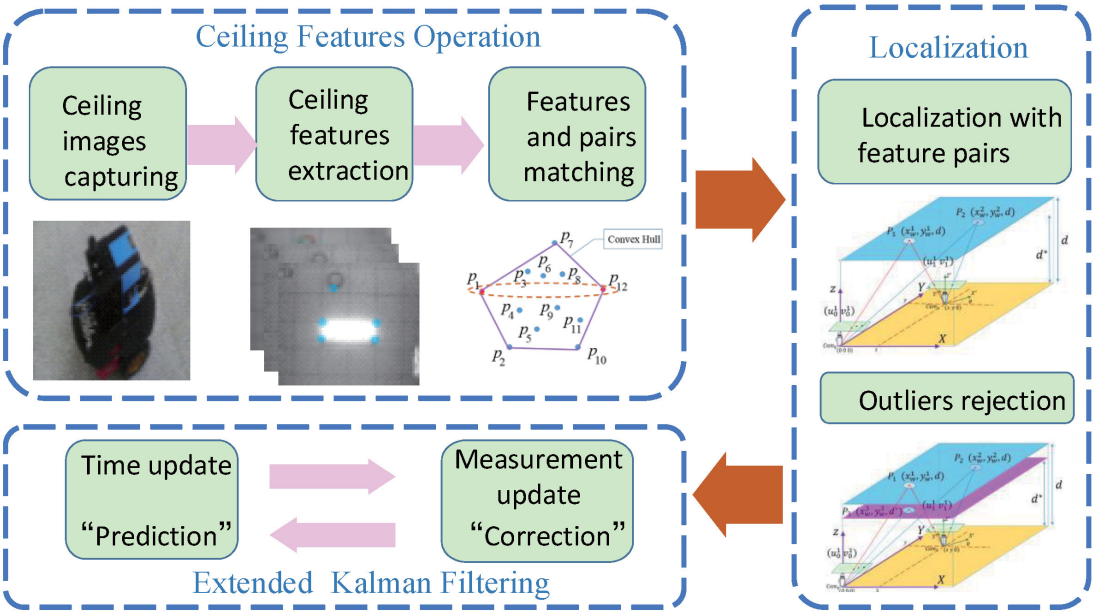

Fig. 1. Framework of the proposed method. It is roughly divided into three steps: (1) ceiling features operation which is consists of ceiling features capturing, ceiling features detection and features and pairs matching; (2) localization with the feature pairs to compute the positioning vector. (3) visual odometry which includes RANSAC and Extended Kalman Filtering.

eras. Therefore, ceiling-view SLAM is less time-demanding than forward-view SLAM. However, the performance of CV-SLAM may degrade due to the lack of landmarks. In this case, the enormous challenge in CV-SLAM is to utilize as much information as possible from only rare landmarks. In addition, real-time performance and positioning accuracy are still the inevitable problems in the localization of indoor service robots.

In this paper, a fast and robust ceiling vision localization framework based on CV-SLAM is proposed, as shown in Fig. 1. The introduced framework aims at home service robots such as cleaning robot effectively, which consists of three parts: ceiling features operation, localization with feature pairs and visual odometry. When a ceiling image is obtained by the looking-upward camera mounted on a robot, the feature extraction part detects the ceiling features and feature pairs are matched using convex hull algorithm. Next, the key issue is how to compute the position vector of a robot. We present a novel position computation algorithm which considers the view-geometric relationships. Finally, the visual odometry which consists of RANSAC and EKF is conducted.

Differing from the existing CV-SLAM, our framework aims to only accomplish the localization task and does not contain the building map. The reasons are that many applications of home service robots only need the position information and motion information instead of the map of environment landmarks. Furthermore, robot which maintains vast redundant landmarks on the ceiling is meaningless. And more importantly, EKF is a popular operation for estimation in many related applications. However, the computational complexity of EKF is equal to the square of the number of landmarks. With the huge numbers of landmarks, the SLAM system using EKF is unable to operate in real-time, and EKF is suitable only for a reasonable number of landmarks that are consistently detected. Accordingly, the proposed framework can enhance the real-time capability effectively.

Another contribution of this paper is that a novel position computation method using feature pairs is proposed and demonstrated. The method can obtain the position information from the feature pairs on the same height, which differs from traditional SLAM [4, 8]. In this case, the position computation process are more simple and effective. Nevertheless, the outliers rejection needs to be added in this method, since few feature pairs exist on the different height.

The rest of this paper is organized as follows. In Section II, more details and deduction for localization with feature pairs are described. Section III presents the other main parts of proposed framework such as distortion model. In Section IV, simulation and real experiments are performed to show the correctness and robustness of our method. Finally, some conclusions is drawn in Section V.

II. Localization with Feature Pairs

In this paper, we put forward a novel localization method with feature pairs which must have the same height on the ceiling. The schematic of localization is illustrated in Fig. 2 (a). In addition, the deduction process of our method in more detail is described below.

A. Notation

For convenience of comprehension, we enumerate two frame of the robot motion which marked as Cam_0 , Cam_1 in Fig. 2 (a). Obviously, the world coordinates

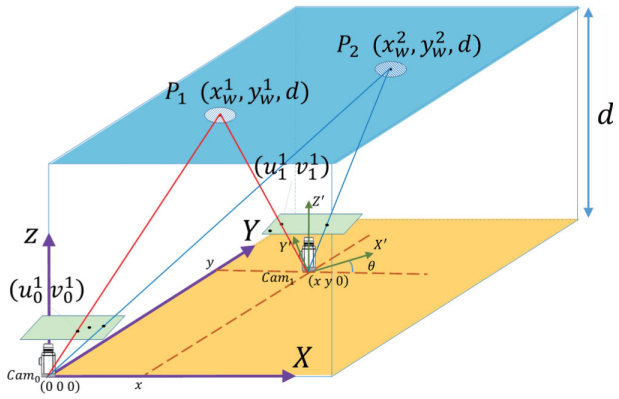

(a) Feature pair on the same height

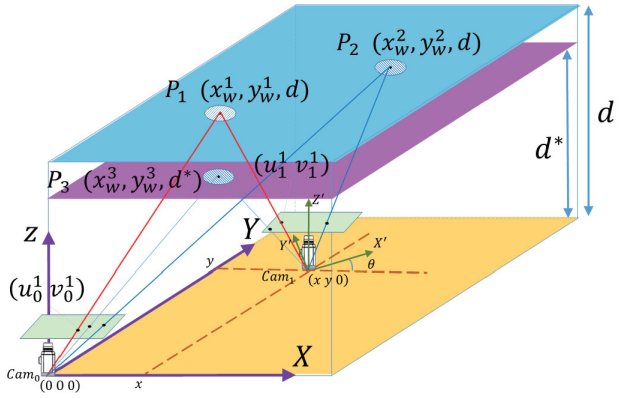

(b) Feature pair on the different height

Fig. 2. View geometry relationship in ceiling vision. In addition to the vast majority of feature pairs such as $< P_1, P_2 >$ in (a) on the same height, rare feature pairs such as $< P_1, P_3 >, < P_2, P_3 >$ in (b) are on the different height.

of points on the ceiling P^1, P^2 are $\begin{bmatrix} x_w^1 & y_w^1 & d \end{bmatrix}^T$ and $\begin{bmatrix} x_w^2 & y_w^2 & d \end{bmatrix}^T$ respectively. Similarly, the world coordinates of Cam_0 and Cam_1 position are $\begin{bmatrix} 0 & 0 & 0 \end{bmatrix}^T$ and $\begin{bmatrix} x & y & 0 \end{bmatrix}^T$. Meanwhile, the rotation matrix of Cam_0 and Cam_1 are $\begin{bmatrix} 0 & 0 & 0 \end{bmatrix}^T$ and $\begin{bmatrix} 0 & 0 & \theta \end{bmatrix}^T$ respectively. On this basis, the intrinsic parameters K of the camera and the extrinsic parameters of Cam_0 and Cam_1 are described as follows:

$$K = \begin{bmatrix} f_u & & u_0 \\ & f_v & v_0 \\ & & 1 \end{bmatrix}, \tag{1}$$

$$\boldsymbol{R}_{cw}^0 = \begin{bmatrix} 1 & & \\ & 1 & \\ & & 1 \end{bmatrix}, \boldsymbol{t}_{cw}^0 = \begin{bmatrix} 0 \\ 0 \\ 0 \end{bmatrix}, \tag{2}$$

$$\begin{aligned} \boldsymbol{R}_{cw}^1 &= \begin{bmatrix} \cos(\theta) & \sin(\theta) & \\ -\sin(\theta) & \cos(\theta) & \\ & & 1 \end{bmatrix}, \\ \boldsymbol{t}_{cw}^1 &= \begin{bmatrix} -\cos(\theta)\, x - \sin(\theta)\, y \\ \sin(\theta)\, x - \cos(\theta)\, y \\ 0 \end{bmatrix}. \end{aligned} \tag{3}$$

Hereby, the localization rroblem resolves itself to compute the positioning vector $\begin{bmatrix} x & y & \theta \end{bmatrix}^T$ under this question.

B. Rigid-body transform from world coordinate

In Fig. 2 (a), it is necessary to obtain the camera coordinates $P_{cam_0}^1$, $P_{cam_1}^1$ of the first feature P^1 from the world coordinate P_w^1 under the camera coordinates system of Cam_0 , Cam_1 respectively. The rigid-body transform process from word coordinate for the first feature is given by:

$$P_{cam_0}^1 = R_{cw}^0 * \left(P_w^1 - \begin{bmatrix} 0 \\ 0 \\ 0 \end{bmatrix} \right) = P_w^1 = \begin{bmatrix} x_w^1 \\ y_w^1 \\ d \end{bmatrix}, \tag{4}$$

$$P_{cam_1}^1 = R_{cw}^1 * \left(P_w^1 - \begin{bmatrix} x \\ y \\ 0 \end{bmatrix} \right) = R_{cw}^1 * \begin{bmatrix} x_w^1 - x \\ y_w^1 - y \\ d \end{bmatrix}. \tag{5}$$

For the second feature, the camera coordinates $P_{cam_0}^2$, $P_{cam_1}^2$ under different frames Cam_0 , Cam_1 can be obtained according to Equation (4), (5).

C. Computing the positioning vector

We regard the first feature and second feature as a feature pair for convenience. Proposed method explains that how to obtain the measurement value of the positioning vector $\begin{bmatrix} x & y & \theta \end{bmatrix}^T$ just with a feature pair. The main step is to obtain the measurement model through formula derivation in the following.

Under the frame Cam_0 , the view-geometric relationship of the intrinsic parameter K , height value d and the first feature $P_{cam_0}^1$ is given by:

$$d * \begin{bmatrix} u_0^1 \\ v_0^1 \\ 1 \end{bmatrix} = K * P_{cam_0}^1 = \begin{bmatrix} f_u & & u_0 \\ & f_v & v_0 \\ & & 1 \end{bmatrix} * \begin{bmatrix} x_w^1 \\ y_w^1 \\ d \end{bmatrix}. \tag{6}$$

It can be simplified into the following equation:

$$\begin{bmatrix} \frac{u_0^1 - u_0}{f_u} \\ \frac{v_0^1 - v_0}{f_v} \end{bmatrix} = \frac{1}{d} * \begin{bmatrix} x_w^1 \\ y_w^1 \end{bmatrix}. \tag{7}$$

Similarly, the relationship for the second feature is given by:

$$\begin{bmatrix} \frac{u_0^2 - u_0}{f_u} \\ \frac{v_0^2 - v_0}{f_v} \end{bmatrix} = \frac{1}{d} * \begin{bmatrix} x_w^2 \\ y_w^2 \end{bmatrix}. \tag{8}$$

Under another frame Cam_1, the view-geometric relationship for the first feature and second feature is expressed in Equation (9) (10) respectively.

$$\begin{bmatrix} \frac{u_1^1 - u_0}{f_u} \\ \frac{v_1^1 - v_0}{f_v} \end{bmatrix} = \frac{1}{d} * \begin{bmatrix} \cos(\theta) & \sin(\theta) \\ -\sin(\theta) & \cos(\theta) \end{bmatrix} * \begin{bmatrix} x_w^1 - x \\ y_w^1 - y \end{bmatrix}, \tag{9}$$

$$\begin{bmatrix} \frac{u_1^2 - u_0}{f_u} \\ \frac{v_1^2 - v_0}{f_v} \end{bmatrix} = \frac{1}{d} * \begin{bmatrix} \cos(\theta) & \sin(\theta) \\ -\sin(\theta) & \cos(\theta) \end{bmatrix} * \begin{bmatrix} x_w^2 - x \\ y_w^2 - y \end{bmatrix}. \tag{10}$$

It could obtain Equation (11) by integrating Equation (7) (8) (9) (10) using elimination which only contains the unknown value θ.

$$\begin{bmatrix} \frac{u_1^1 - u_1^2}{f_u} \\ \frac{v_1^1 - v_1^2}{f_v} \end{bmatrix} = \begin{bmatrix} \cos(\theta) & \sin(\theta) \\ -\sin(\theta) & \cos(\theta) \end{bmatrix} \begin{bmatrix} \frac{u_0^1 - u_0^2}{f_u} \\ \frac{v_0^1 - v_0^2}{f_v} \end{bmatrix} \tag{11}$$

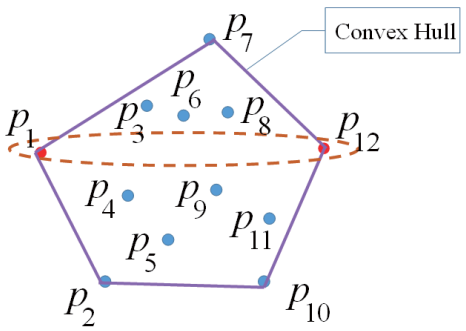

Fig. 3. Matching feature pairs using convex hull algorithm

In this manner, Kabsch algorithm [19] can be employed to solve Equation (11). With the θ, vector $[x, y]$ can be obtain by plugged into the existing equation such as Equation (9) with ease.

III. Localization Framework

Except the localization with feature pairs, other skills of proposed framework shown in Fig. 1 are illustrated as follows:

A. Distortion Model

Naturally, wide angle images can be obtained from fish-eye lenses or catadioptric cameras. Unavoidably, we require to get the real images from the distorted images with distortion model. The Field of View (FoV) model [14] is utilized in our framework. Undistorted image coordinates (p, q) are computed by the mapping $(i_d, j_d) \leftarrow (p, q)$ expressed in Equation (12), (13).

$$r_u = \sqrt{p^2 + q^2}, r_d = \frac{1}{\omega} \arctan(2r_u \tan\frac{\omega}{2}) \tag{12}$$

$$\begin{bmatrix} i_d \\ j_d \end{bmatrix} = \frac{r_d}{r_u} \begin{bmatrix} p \\ q \end{bmatrix} \tag{13}$$

B. Matching feature pairs

According to the view-geometric relationship, feature pairs whose relative positions are shorter such as $< p_4, p_6 >$ shown in Fig. 3 in ceiling images are more sensitive to noise in the localization process. To enhance the correctness, a greedy algorithm is presented in Algorithm 1 to detect the longest feature pairs such as $< p_1, p_{12} >$ in Fig. 3.

Next, Melkman's convex hull algorithm [21] are applied in Algorithm 1 to check for the longest distance feature pair, and the time complexity of Algorithm 1 is $O(n)$.

Algorithm 1 Matching feature pairs

Require: Features set $P = \{p_1, p_2, ..., p_n\}$, feature p_i.
Ensure: Feature pairs set G.
1: Source set $S_P = \{< p_i, p_j > | i < j, p_i \in P, p_j \in P\}$
2: Goal set $G \leftarrow \phi$
3: **for** each point pair$< p_i, p_j > \in S_P$ **do**
4: Select the longest distance point pair $< p_m, p_n >$ with the convex hull algorithm
5: $G \leftarrow G \bigcup \{< p_m, p_n >\}$
6: $P \leftarrow P - \{p_m, p_n\}$
7: $S_P = \{< p_i, p_j > | i < j, p_i \in P, p_j \in P\}$
8: **end for**

C. Outliers rejection

In section II, we take full advantage of two features at the same height on the ceiling as the information about structure of the world around the robot to position itself. However, the ceiling relative to ground is not parallel plane entirely on rare occasion. Under this circumstance, there are outliers which are not at the same height with other features on the ceiling such as P_3 in the Fig. 2 (b). Therefore, it is necessary to distinguish and reject these outliers at the last step to maintain the position accuracy of our method.

As to this, we adopt the homography decomposition technique [20] to verify the chosen features and to accomplish the outliers rejection.

D. EKF based Localization

As in most existing framework, an EKF will be utilized in our framework. In this case, the localization problem becomes a stochastic estimation problem with EKF.

Probabilistic Map Representation: The state vector maintains the position information $\begin{bmatrix} x_r(k) & y_r(k) \end{bmatrix}^T$ and the orientation $\theta_r(k)$ and the motion information $\begin{bmatrix} v_x(k) & v_y(k) & \omega(k) \end{bmatrix}^T$, expressed by

$$\xi(k) = \begin{bmatrix} x_r(k) & y_r(k) & \theta_r(k) & v_x(k) & v_y(k) & \omega(k) \end{bmatrix}^T, \tag{14}$$

in which k is the discrete time index. Remarkably, the state vector excludes the information of environment features on the ceiling images.

Motion Model: The constant velocity is employed as the motion model in the framework as suggested in [4]. However, we will take the noise of process $\boldsymbol{n}(k) = \begin{bmatrix} n_x(k) & n_y(k) & o_\omega(k) \end{bmatrix}^T$ into consideration. Hereby, the state update produced is:

$$\xi(k+1) = \begin{bmatrix} x_r(k) + (v_x(k) + n_x(k)) * \Delta t \\ y_r(k) + (v_y(k) + n_y(k)) * \Delta t \\ \theta_r(k) + (\omega_x(k) + o_\omega(k)) * \Delta t \\ v_x(k) + n_x(k) \\ v_y(k) + n_y(k) \\ \omega(k) + o_\omega(k) \end{bmatrix}. \tag{15}$$

Measurement Model: Measurement model is the projection function, which projects the features on the ceiling to the sensor observation. And the measurement model of localization EKF process is given by:

$$\begin{bmatrix} p \\ q \end{bmatrix} = \begin{bmatrix} \frac{u-u_0}{f_u} \\ \frac{v-v_0}{f_v} \end{bmatrix} = \frac{1}{d} \begin{bmatrix} \cos(\theta) & \sin(\theta) \\ -\sin(\theta) & \cos(\theta) \end{bmatrix} \begin{bmatrix} x_w - x \\ y_w - y \end{bmatrix}. \tag{16}$$

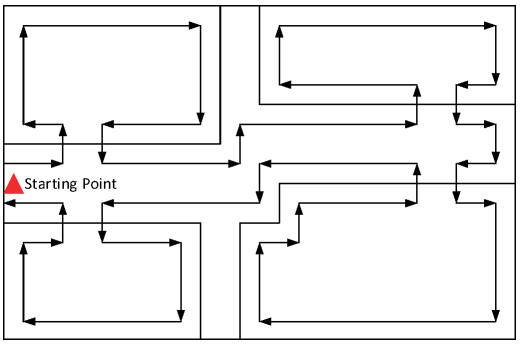

(a) Simulation environment and path

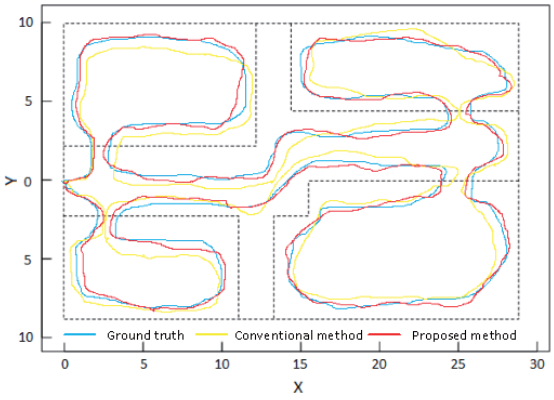

(b) Simulation results depicted by the trajectories

Fig. 4. Simulation experimentation.

IV. Experiments and Discussions

A. Simulation experiments

To evaluate our method, localization algorithms are simulated in a noisy environment. Simulation environment which consists of a corridor and four rooms is depicted in Fig. 4 (a), and the robot starts at the triangle in the map and travels along the arrows and finishes at the starting point. The simulation results of both the conventional method [9] and our method are compared in Fig. 4 (b). The blue line are from the ground truth of the map, while the yellow line and the red line represent the trajectories estimated by the conventional method and the proposed method respectively.

Around the starting point of triangle, the trajectories are almost consistent with the ground truth. Nevertheless, the lines deviate from the ground truth with the robot explores further, and the proposed method can keep track of the ground truth more better compared with the conventional method [9].

To verify the results in statistic, 50 independent runs are performed with the four different noise conditions. The performance of localization methods is computed by:

$$e_{trj} = \frac{1}{M}\sum_{m=1}^{M}\left(\frac{1}{T}\sum_{t=1}^{T}\sqrt{(\hat{r}_{x,t}^{m} - r_{x,t}^{m})^2 + (\hat{r}_{y,t}^{m} - r_{y,t}^{m})^2}\right), \tag{17}$$

where M is the number of the independent runs, $(r_{x,t}^{m}, r_{y,t}^{m})$ is the ground truth coordinate and $(\hat{r}_{x,t}^{m}, \hat{r}_{y,t}^{m})$ is the evaluated position at time t in the mth trial.

The statistical results of simulation are shown in TABLE I. Here, M_{noise} presents the noise covariance matrices of measurement in the simulation, and the second column and third column represent the localization errors with the conventional method [9] and proposed method under different noise condition respectively. The performance comparison of both methods is depicted in the last column. Naturally, the proposed method outperforms the conventional method in reduced errors form TABLE I.

TABLE I

Statistical results of simulation

M_{noise}	Conventional method [1]	Proposed method	Promotion (%)
$\begin{bmatrix}1 & 0\\ 0 & 0.1\end{bmatrix} \times 0.01$	3.313	2.403	27.46
$\begin{bmatrix}1 & 0\\ 0 & 0.1\end{bmatrix} \times 0.02$	6.902	2.613	62.14
$\begin{bmatrix}1 & 0\\ 0 & 0.1\end{bmatrix} \times 0.03$	6.874	2.935	57.30
$\begin{bmatrix}1 & 0\\ 0 & 0.1\end{bmatrix} \times 0.04$	7.563	2.769	63.38

B. Real experiments

Some real experiments are conducted to show the effectiveness of our method. As shown in Fig. 5 , the proposed algorithm is applied to a Pioneer 3DX in office environment. The computer on Pioneer 3DX has a Pentium III 800 MHz CPU and 512M memory. The camera mounted on the Pioneer 3DX is IMAVISION V10 camera with the wide-angle lens of 160° and 640×480 image resolution. The test environment consists of a corridor and two rooms, and the size of the test environment is $6m \times 15m$ as shown in Fig. 5. The robot starts at the triangle in the map and travels along the arrows in the floor plan.

In real experiments, the localization results of different methods are compared such as conventional method [9, 10, 12] and the proposed method. The localization performance of the methods is measured by:

$$e_{trj} = \frac{1}{T}\sum_{t=1}^{T}\sqrt{(\hat{r}_{x,t} - r_{x,t})^2 + (\hat{r}_{y,t} - r_{y,t})^2}, \tag{18}$$

where $(\hat{r}_{x,t}, \hat{r}_{y,t})$ is the estimated position of the robot by the methods at time t and $(r_{x,t}, r_{y,t})$ is the ground-truth received by the laser sensor of the Pioneer 3DX.

TABLE II

Real experimentation results

Methods	Trajectory errors (cm)	Time complexity
Jeong Method [1]	98.32	$O(MN^2)$
Frintrop Method [2]	85.34	$O(MN^2)$
Choi Method [3]	80.12	$O(MN^2)$
Proposed method	**77.89**	$\boldsymbol{O(MN)}$

(a)

(b)

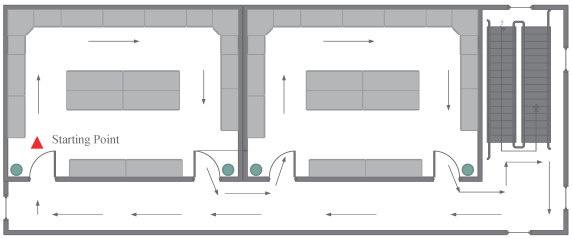

(c)

Fig. 5. Test environment: (a) corridor, (b) the room (c) floor plan

In TABLE II, the experimental results are summarized. Proposed method outperforms the other existing methods such as [9, 10, 12]. However, our method does not have the huge advantages compared with others in the correctness of localization. According to TABLE II, the time complexity of proposed method is only $O(MN)$, which is much better than others' $O(MN^2)$, where M is the number of observed measurements at the time slot and N is the number of ceiling features. The reason is that the state vector of EKF in our framework only contains the position information and motion information, which does not maintain the features in excess. By contrast, it has been shown that the correctness of localization is not reduced without the entire map of ceiling features in our framework. In this manner, it can enhance the real-time performance.

V. Conclusions

The contribution of this paper lies in a novel framework of the fast and efficient localization for home service robots. Moreover, the localization method is proposed which is based on feature pairs in ceiling vision. In experiments, simulation and real experimental results have shown that proposed framework can be put into practise to enhance the correctness and real-time performance. However, the obtained results depend on that the ceiling are parallel to the ground in general. In the future work, the boundary lines and boundary landmarks will be added in the positioning method, and the experiments will be conducted in a large indoor and noisy environments.

References

[1] D. Nister, O. Naroditsky and J. Bergen, "Visual odometry for ground vehicle applications," *Journal of Field Robotics*, vol. 23 no. 3, pp. 3-20, 2006.

[2] H. D. Whyte and T. Bailey, "Simulataneous localization and mapping:part 1," *IEEE Robotics and Automation Magazine*, vol. 13, no. 2, pp. 99-110, 2006.

[3] R. Smith, M. Self, P. Cheeseman, "Estimating uncertain spatial relationships in robotics," *Autonomous Robot Vehicles: Springer*, vol. 29, pp. 167-193, 1990.

[4] A. J. Davision, I. D. Reid, N. D. Molton and Olivier Stasse, "MonoSLAM: Real-Time Single Camera SLAM," *IEEE Transactions on Pattern Analysis and Machine Intelligence (PAMI)*, vol. 29, no. 6, pp. 1052-1067, 2007.

[5] A. Kawewong, N. Tongprasit, S. Tangruamsub, O. Hasegawa, "Online and incremental appearance-base SlAM in highly dynamic environments," *International Journal of Robotics Research (IJRR)*, vol. 30, no. 1, pp. 33-35, 2011.

[6] B. Steder, G. Grisetti, C. Stachniss, W. Burgard, "Visual SLAM for flying vehicles," *IEEE Transactions on Robotics*, vol. 24, no. 5, pp. 1088-1093, 2008.

[7] H. Kretzschmar, C. Stachniss, "Informationtheoretic compression of pose graphs for laser-based SLAM," *Int. Journal of Robotics Research (IJRR)*, vol. 31, no. 11, pp. 1219-1230, 2012.

[8] S. Y. Hwang, J. B. Song, "Monocular vision based SLAM in indoor environment using corner, lamp, and door features from upward-looking camera," *IEEE Trans. on Industrial Electronics*, vol.58(10), pp. 4804-4812, 2011.

[9] W. Y. Jeong and K. M. Lee, "Visual SLAM with line and corner features," *IEEE/RSJ Int. Conf. on Intelligent Robots and Systems (IROS)*, pp. 2570-2575, 2006.

[10] S. Frintrop, P. Jensfelt, "Attentional landmarks and active gaze control for visual SLAM," *IEEE Trans. on Robotics*, vol. 24, no. 5, pp. 1054-1065, 2008.

[11] J. Civera, A. J. Davison, J. Montiel, "Inverse depth parametrization for monocular SLAM," *IEEE Trans. on Robotics*, vol. 24, no. 5, pp. 932-945, 2008

[12] H. Choi, D. Y. Kim, J. P. Hwang, C. W. Park and E. Kim, "Efficient simultaneous localization and mapping based on ceiling-view: ceiling boundary feature map approach," *Advanced Robotics*, vol. 26, no. 5-6, pp. 653-671, 2012.

[13] D. Y. Kim, H. Choi, H. Lee, E. Kim, "A new cvSLAM exploiting a partially known landmark association," *Advanced Robotics*, vol. 27, no. 14, pp. 1073-1086, 2013.

[14] F. Devernay and O. Faugeras, "Straight lines have to be straight," *Machine Vision and Applications*, vol. 13, no. 1, pp. 14-24, 2001.

[15] W. Y. Jeong and K. M. Lee, "CV-SLAM: a new ceiling vision based SLAM tennique," *IEEE/RSJ Int. Conf. on Intelligent Robots and Systems*, pp. 3195-3200, 2005.

[16] D. Xu, L. Han, M. Tan, and Y. F. Li, "Ceiling-based visual positioning for an indoor mobile robot with monocular vision," *IEEE Trans.on Industrial Electronics*, vol. 56, no. 5, pp. 1617-1628, 2009.

[17] De Souza, N. Guilherme, C. Acinash, "Vision for Mobile Robot Navigation: A Survey," *IEEE Trans. on Pattern Analysis and Machine Intelligence (PAMI)*, vol. 24, no. 5, pp. 237-267, 2002.

[18] S. Y. Hwang and J. B. Song, "Monocular Vision-based Global Localization Using Position and Orientation of Ceiling Features," *IEEE Int. Conf. on Robotics and Automation (ICRA)*, pp. 3785-3790, 2013.

[19] W. Kabsch, "A solution for the best rotation to relate two sets of vectors," *Acta Crystallographica Section A*, vol. 32, no. 5, pp. 922-923, 1976.

[20] O. Faygeras and F. Lustman, "Motion and structure from motion in a piecewise planar environment," *Int. Journal of Pattern Recognition and Artificial Intelligence*, vol. 2, no. 3, pp. 485-508, 1988.

[21] A. A. Melkman, "On-line construction of the convex hull of a simple polyline," *Information Processing Letters*, vol. 25, no. 1, pp. 11-12, 1987.